of the circadian cycle in mammals. Mutational analyses of other putative clock genes will be essential for unravelling the molecular mechanisms underlying the mammalian circadian clock. These mutants will also provide useful animal models for elucidating the aetiology of and developing treatments for disorders in humans related to the sleep–wake cycle. □

Methods

Generation of *mPer2*^{Brdm1} mutant mice. We isolated a genomic clone from a mouse 129S5/SvEvBrd genomic library using a mouse *mPer2* complementary DNA probe. A targeting vector was constructed with *PGK-Neo* as the positive selection marker and *HSVtk* as the negative selection marker to delete a 2.1-kilobase (kb) fragment. We used a 6.7-kb *Bgl*II fragment as the 5′ homology region and a 4.0-kb *Kpn*I fragment as the 3′ homology region. The *HSVtk*, *PGK-Neo* and vector backbone were from pKO SelectTK, pKO SelectNeo V800 and pKO Scrambler V924 (Lexicon Genetics). Tissue culture, electroporation, mini-Southern blot analysis on embryonic stem cell colonies, generation of chimaeric and germline mice and tail DNA genotyping were done as described[27,28].

Locomotor activity monitoring and circadian phenotype analysis. Mice were housed in individual cages equipped with a running wheel in ventilated, light-tight chambers with controlled lighting. Wheel-running activity was monitored by an on-line PC using the Chronobiology Kit (Stanford Software Systems). In the LD cycle, the light was turned on at 7:00 (ZT 0) and off at 19:00 (ZT 12). The switch into constant darkness (DD) was effected by not turning on the light at the usual time. The activity records are double plotted so that each day/cycle's activity is shown both to the right and below that of the previous day/cycle. Activity is plotted in density percentile distribution (Fig. 2) or threshold (Fig. 3) format. For activity counting we used the ACTCNT program of the Chronobiology Kit. To determine the period length, an interval with a 10-day minimum during which the circadian period appeared to be stable on the activity record was analysed with a χ^2 periodogram[29] using the Stanford Chronobiology Kit. We used Fourier periodogram analysis[15] in the Chronobiology Kit to assess the strength of circadian and/or ultradian rhythmicity.

***In situ* hybridization.** Mice were killed by cervical dislocation under ambient light conditions at ZT 6 and ZT 12 and under a 15 W safety red light at ZT 18 and ZT 0/24. Specimen preparation and *in situ* hybridization with an *mPer1* and an *mPer2* probe were carried out as described[4,30]. The *mPer2* probe is outside the region deleted in the mutant. The *mPer3* probe was made from an RT–PCR product corresponding to nucleotides 480–824 (AF050182). The *Clock* probe was made from an RT–PCR product corresponding to nucleotides 1352–2080 (AF000998). Tissue was visualized by fluorescence of Hoechst dye-stained nuclei (blue in Fig. 4).

Northern blot and RT-PCR analysis. Tissues were collected and frozen in liquid nitrogen and stored at −80 °C. RNA was prepared with the RNAzol™ B RNA isolation kit (TEL-TEST). We performed northern blot analysis on total tissue RNA using denaturing formaldehyde gel. For RT–PCR analysis, first strand cDNA was generated using Moloney reverse transcriptase (BRL-GIBCO) and oligo dT-priming from total liver RNA. An aliquot of the first strand cDNA was then amplified by PCR across the deletion region with the 5′ primer CTA CCT GGT CAA GGT GCA AGA G and the 3′ primer GGT TTG AAT CTT GCC ACT GG. The RT–PCR products were then sequenced with an internal primer AGG GTA CAC TCG GGC TAT GA.

Received 31 December 1998; accepted 18 May 1999.

1. Pittendrigh, C. S. Temporal organization: reflections of a Darwinian clock-watcher. *Annu. Rev. Physiol.* **55,** 16–54 (1993).
2. Sun, Z. S. *et al. RIGUI*, a putative mammalian ortholog of the *Drosophila period* gene. *Cell* **90,** 1003–1011 (1997).
3. Tei, H. *et al.* Circadian oscillation of a mammalian homologue of the *Drosophila period* gene. *Nature* **389,** 512–516 (1997).
4. Albrecht, U., Sun, Z. S., Eichele, G. & Lee, C. C. A differential response of two putative mammalian circadian regulators, *mper1* and *mper2*, to light. *Cell* **91,** 1055–1064 (1997).
5. Shearman, L. P., Zylka, M. J., Weaver, D. R., Kolakowski, L. F. Jr & Reppert, S. M. Two *period* homologs: circadian expression and photic regulation in the suprachiasmatic nuclei. *Neuron* **19,** 1261–1269 (1997).
6. Takumi, T. *et al.* A new mammalian *period* gene predominantly expressed in the suprachiasmatic nucleus. *Genes Cells* **3,** 167–176 (1998).
7. Zylka, M. J., Shearman, L. P., Weaver, D. R. & Reppert, S. M. Three *period* homologs in mammals: differential light responses in the suprachiasmatic circadian clock and oscillating transcripts outside of brain. *Neuron* **20,** 1103–1110 (1998).
8. Takumi, T. *et al.* A light-independent oscillatory gene *mPer3* in mouse SCN and OVLT. *EMBO J.* **17,** 4753–4759 (1998).
9. Huang, Z. J., Edery, I. & Rosbash, M. PAS is a dimerization domain common to *Drosophila* Period and several transcription factors. *Nature* **364,** 259–262 (1993).
10. Crosthwaite, S. K., Dunlap, J. C. & Loros, J. J. *Neurospora wc-1* and *wc-2*: transcription, photo-responses, and the origins of circadian rhythmicity. *Science* **276,** 763–769 (1997).
11. King, D. P. *et al.* Positional cloning of the mouse circadian *Clock* gene. *Cell* **89,** 641–653 (1997).
12. Rutila, J. E. *et al.* CYCLE is a second bHLH-PAS clock protein essential for circadian rhythmicity and transcription of *Drosophila period* and *timeless*. *Cell* **93,** 805–814 (1998).
13. Allada, R., White, N. E., So, W. V., Hall, J. C. & Rosbash, M. A mutant *Drosophila* homolog of mammalian *Clock* disrupts circadian rhythms and transcription of *period* and *timeless*. *Cell* **93,** 791–804 (1998).
14. Ponting, C. P. & Aravind, L. PAS: a multifunctional domain family comes to light. *Curr. Biol.* **7,** R674–R677 (1997).
15. Bracewell, R. N. *The Hartley Transform* (Oxford Univ. Press, New York, 1986).
16. Aschoff, J. in *Handbook of Behavioral Neurobiology 4: Biological Rhythms* (ed. Aschoff, J.) 3–10 (Plenum, New York, 1981).
17. Ibuka, N., Inouye, S. I. & Kawamura, H. Analysis of sleep-wakefulness rhythms in male rats after suprachiasmatic nucleus lesions and ocular enucleation. *Brain Res.* **122,** 33–47 (1977).
18. Vitaterna, M. H. *et al.* Mutagenesis and mapping of a mouse gene, *Clock*, essential for circadian behavior. *Science* **264,** 719–725 (1994).
19. Dowse, H. B. & Ringo, J. M. Further evidence that the circadian clock in *Drosophila* is a population of coupled ultradian oscillators. *J. Biol. Rhythms* **2,** 65–76 (1987).
20. Hamblen-Coyle, M. J., Wheeler, D. A., Rutila, J. E., Rosbash, M. & Hall, J. C. Behavior of period-altered rhythm mutants of *Drosophila* in light:dark cycles. *J. Insect Behav.* **5,** 417–446 (1992).
21. Ralph, M. R. & Menaker, M. A mutation of the circadian system in golden hamsters. *Science* **241,** 1225–1227 (1988).
22. Hardin, P. E., Hall, J. C. & Rosbash, M. Feedback of the *Drosophila period* gene product on circadian cycling of its messenger RNA levels. *Nature* **343,** 536–540 (1990).
23. Dunlap, J. C. Genetics and molecular analysis of circadian rhythms. *Annu. Rev. Genet.* **30,** 579–601 (1996).
24. Balsalobre, A., Damiola, F. & Schibler, U. A serum shock induces circadian gene expression in mammalian tissue culture cells. *Cell* **93,** 929–937 (1998).
25. Sangoram, A. M. *et al.* Mammalian circadian autoregulatory loop: A *Timeless* ortholog and *mPer1* interact and negatively regulate CLOCK-BMAL1-induced transcription. *Neuron* **21,** 1101–1113 (1998).
26. Bae, K., Lee, C., Sidote, D., Chuang, K. Y. & Edery, I. Circadian regulation of a *Drosophila* homolog of the mammalian *Clock* gene: PER and TIM fucntion as positive regulators. *Mol. Cell. Biol.* **18,** 6142–6151 (1998).
27. Matzuk, M. M., Finegold, M. J., Su, J. G., Hsueh, A. J. & Bradley, A. Alpha-inhibin is a tumour-suppressor gene with gonadal specificity in mice. *Nature* **360,** 313–319 (1992).
28. Ramirez-Solis, R., Davis, A. C. & Bradley, A. Gene targeting in embryonic stem cells. *Methods Enzymol.* **225,** 855–878 (1993).
29. Sokolove, P. G. & Bushell, W. N. The chi square periodogram: its utility for analysis of circadian rhythms. *J. Theor. Biol.* **72,** 131–160 (1978).
30. Albrecht, U., Eichele, G., Helms, J. A. & Lu, H. in *Molecular and Cellular Methods in Developmental Toxicology* (ed. Daston, G. P.) 23–48 (CRC Press, Boca Raton, FL, 1997).

Supplementary information is available on *Nature*'s World-Wide Web site (http://www.nature.com) or as paper copy from the London editorial office of *Nature*.

Acknowledgements. We thank S. Vaishnav, L. Qiu, Y.-C. Cheah, E. Sheppeard and S. Rivera for technical assistance; P. Hastings for comments on the manuscript; J. W. Patrick for providing space and facilities for circadian phenotype analysis; and J. Takahashi, Y. Zhao and M. Bucan for helpful discussions. This work was supported by grants from NINDS and NIDA to J. W. Patrick, from the Max-Planck Society to G. E., from NIH and the Department of Defense to C.C.L., and from NIH and the Howard Hughes Medical Institute to A.B. A.B. is an investigator with HHMI.

Correspondence and requests for materials should be addressed to C.C.L. (e-mail: ching@bcm.tmc.edu)

Immunization with amyloid-β attenuates Alzheimer-disease-like pathology in the PDAPP mouse

Dale Schenk, Robin Barbour, Whitney Dunn, Grace Gordon, Henry Grajeda, Teresa Guido, Kang Hu, Jiping Huang, Kelly Johnson-Wood, Karen Khan, Dora Kholodenko, Mike Lee, Zhenmei Liao, Ivan Lieberburg, Ruth Motter, Linda Mutter, Ferdie Soriano, George Shopp, Nicki Vasquez, Christopher Vandevert, Shannan Walker, Mark Wogulis, Ted Yednock, Dora Games & Peter Seubert

Elan Pharmaceuticals, 800 Gateway Boulevard, South San Francisco, California 94080, USA

Amyloid-β peptide (Aβ) seems to have a central role in the neuropathology of Alzheimer's disease (AD)[1]. Familial forms of the disease have been linked to mutations in the amyloid precursor protein (APP) and the presenilin genes[2,3]. Disease-linked mutations in these genes result in increased production of the

42-amino-acid form of the peptide ($A\beta_{42}$)[4–8], which is the predominant form found in the amyloid plaques of Alzheimer's disease[9,10]. The PDAPP transgenic mouse, which overexpresses mutant human APP (in which the amino acid at position 717 is phenylalanine instead of the normal valine), progressively develops many of the neuropathological hallmarks of Alzheimer's disease in an age- and brain-region-dependent manner[11,12]. In the present study, transgenic animals were immunized with $A\beta_{42}$, either before the onset of AD-type neuropathologies (at 6 weeks of age) or at an older age (11 months), when amyloid-β deposition and several of the subsequent neuropathological changes were well established. We report that immunization of the young animals essentially prevented the development of β-amyloid-plaque formation, neuritic dystrophy and astrogliosis. Treatment of the older animals also markedly reduced the extent and progression of these AD-like neuropathologies. Our results raise the possibility that immunization with amyloid-β may be effective in preventing and treating Alzheimer's disease.

Our initial experiments investigated the effects of immunization against amyloid-plaque-related proteins on the development of AD-like neuropathology in young PDAPP mice, in which treatment had begun before the occurrence of significant plaque pathology (6 weeks of age). The immunogens were either synthetic human $A\beta_{42}$, the major component of β-amyloid plaques in AD and PDAPP mice, or peptides derived from the primary amino-acid sequence of serum amyloid-P component (SAP). SAP is a protein associated with amyloid plaques in AD and other amyloid diseases[13]. Two additional groups of PDAPP mice were immunized with PBS buffer or were left untreated to serve as controls. Mice received 11 immunizations over an 11-month period. We found that eight of nine PDAPP mice immunized with $A\beta_{42}$ developed and maintained serum antibody titres against $A\beta_{42}$ of greater than 1:10,000. The ninth mouse had a lower titre, of approximately 1:1,000. Cross-reactivity of the antisera was also observed against mouse amyloid-β peptide, although titres were generally an order of magnitude lower. Mice immunized with SAP peptides had antibody titres against SAP ranging from 1:1,000 to 1:10,000, with the exception of one mouse which had a titre greater than 1:10,000 (data not shown). Control animals receiving adjuvant alone had negligible titres to $A\beta_{42}$. At 13 months of age, quantitative immunohistochemical measures determined the extent of amyloid-β burden and the prevalence of neuritic plaques, astrogliosis and microgliosis.

Immunization with $A\beta_{42}$ resulted in almost complete prevention of amyloid-β deposition (Figs 1, 2). Seven of nine mice immunized with $A\beta_{42}$, including the mouse with the lowest anti-Aβ titre, had no detectable amyloid-β deposits in their brains. One mouse from this treatment group had a single isolated plaque in the six brain sections examined, whereas a second animal had a greatly reduced amyloid-β burden. Quantitative imaging of the amyloid-β burden in the hippocampus verified the near-total reduction achieved in $A\beta_{42}$-treated animals (Fig. 1). The median values of the amyloid-β burden for the PBS group (2.22%) and for the untreated control group (2.65%) were significantly greater than that of the Aβ-immunized group (0.00%, $P = 0.0005$). In contrast, the median value of amyloid-β for the group immunized with SAP peptides (5.74%), although increased, was not significantly different from that of control animals. Brain tissue from the PBS-treated control mice contained numerous amyloid-β deposits in the hippocampus (Fig. 2) and retrosplenial cortex (not shown). We observed a similar pattern of amyloid-β deposition in mice immunized with SAP peptides. Brain sections from $A\beta_{42}$-immunized mice were also stained with thioflavin S to rule out the possibility that the lack of immunohistochemically detectable plaques was due to competition by the *de novo* anti-Aβ antibodies produced by these animals (see below). Thioflavin S detected no amyloid-β deposits in these $A\beta_{42}$-immunized mice (not shown). In contrast, immunization with SAP peptides did not affect amyloid-β deposition, suggesting that

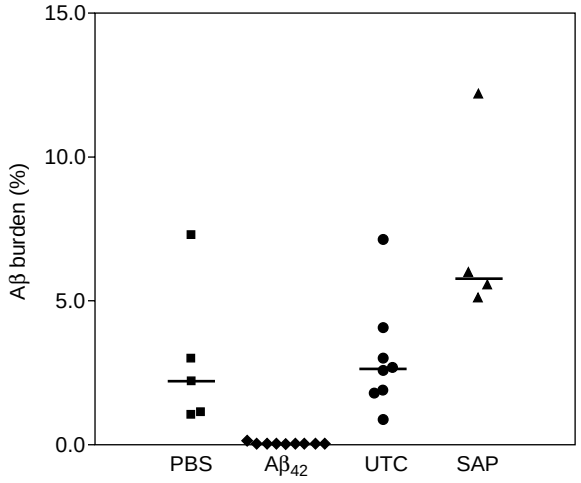

Figure 1 Reduction of Aβ burden in the hippocampus at 13 months of age in mice immunized with $A\beta_{42}$. PDAPP mice were immunized beginning at 6 weeks of age as described in Methods. The percentage of the area of the hippocampal region occupied by Aβ deposits was determined by quantitative image analysis. Values for individual mice are shown sorted by treatment group. Horizontal lines represent the median values. The $A\beta_{42}$-immunized group had significantly fewer Aβ deposits than any of the other three groups ($P = 0.001$), which are not significantly different from each other ($P > 0.05$). UTC, untreated controls; SAP, mice immunized with serum amyloid P.

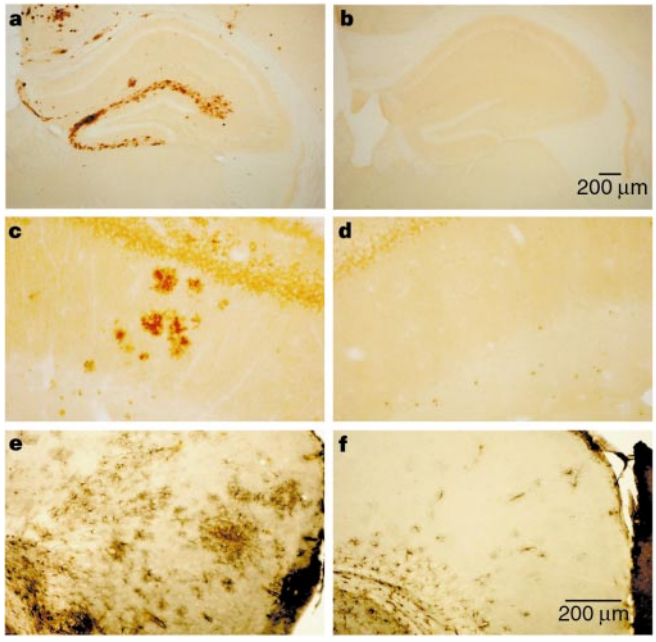

Figure 2 Hippocampal Aβ deposition, neuritic plaque formation and cortical astrocytosis in PBS- and $A\beta_{42}$-injected mice. Images from 13-month-old mice with Aβ burdens representative of the median values (see Fig. 1) of their respective groups are shown. **a**, **b**, Hippocampal Aβ plaques in PBS- (**a**) and $A\beta_{42}$-injected (**b**) mice. **a** shows abundant Aβ deposition in the outer molecular layer of the hippocampal dentate gyrus of a PBS-treated animal. **b** shows no detectable Aβ in this region of an $A\beta_{42}$-immunized mouse, a profile observed in most animals from this group. Scale bar in **b** corresponds to both **a** and **b**. **c**, **d**, Hippocampal sections from PBS- (**c**) and $A\beta_{42}$-injected (**d**) mice. Typical dystrophic neurites associated with neuritic plaques and labelled with the APP-specific monoclonal antibody 8E5 (ref. 16) were found in PBS- (**c**), but not $A\beta_{42}$-injected animals (**d**). **e**, **f**, Abundant plaque-associated astrocytosis, as determined by GFAP immunohistochemistry (Sigma), was evident in the retrosplenial cortex of PBS- (**e**) but not $A\beta_{42}$-injected (**f**) mice. Scale bar in **f** corresponds to **c**–**f**.

immune responses against plaque components *per se* are insufficient to prevent or eliminate β-amyloid plaques and neuropathology.

The brains of $A\beta_{42}$-treated mice that contained no amyloid-β deposits were also devoid of the dystrophic neurites that characterize the neuritic plaques (Fig. 2: compare c and d). Small numbers of dystrophic neurites were present in the two $A\beta_{42}$-treated mice that had detectable Aβ deposits. In contrast, all brains from SAP-injected mice and the two control groups (PBS-injected and untreated mice) had numerous neuritic plaques. Image analyses of the hippocampus demonstrated the virtual elimination of dystrophic neurites in the $A\beta_{42}$-treated mice (median, 0.00%) compared with the PBS recipients (median, 0.28%; $P = 0.0005$).

Astrocytosis, another hallmark of plaque-associated pathology in both Alzheimer's disease and PDAPP mice, was dramatically reduced in the brains of all of the $A\beta_{42}$-injected mice (Fig. 2). Brains from mice in all other groups contained numerous clusters of astrocytes that were immunoreactive to glial fibrillary acidic protein (GFAP), a finding typical of Aβ-plaque-associated gliosis (Fig. 2e).

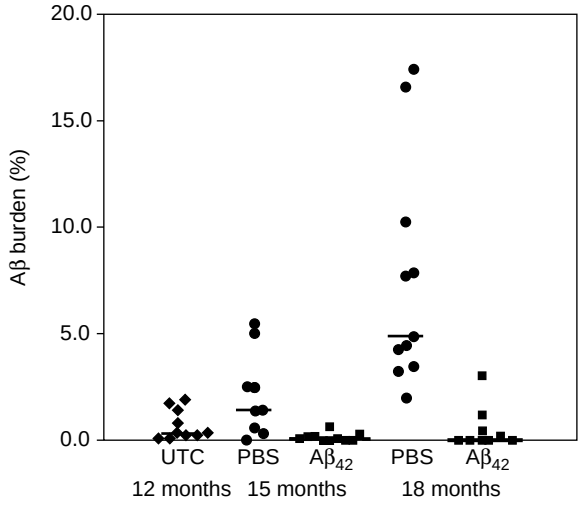

Figure 3 Quantitative image analysis of the cortical Aβ burden in older PBS- and Aβ-treated mice. Immunization of PDAPP mice was begun at 11 months of age. Amyloid burden was significantly reduced in the $A\beta_{42}$ group compared with the PBS controls at both 15 ($P = 0.003$) and 18 ($P = 0.0002$) months of age. The median value of the amyloid burden for each group is shown by the horizontal lines.

Association of amyloid plaques and reactive astrocytes was verified in a subset of GFAP-reacted sections counterstained with thioflavin S. The results of image analyses for the retrosplenial cortex verified that the reduction in astrocytosis was significant, with a median value of 1.55% for mice immunized with $A\beta_{42}$ compared with median values of greater than 6% for groups immunized with SAP peptide or PBS, or untreated control mice ($P = 0.0017$).

Sections of the mouse brains were also reacted with a monoclonal antibody specific for MAC-1 (CD11b; Chemicon), a cell-surface marker that is upregulated on activated, plaque-associated microglia. MAC-1 labelling was substantially lower in the brains of mice treated with $A\beta_{42}$ compared with the PBS control group, a finding consistent with the lack of a plaque-induced gliosis (not shown).

The almost complete absence of plaques in the brains of $A\beta_{42}$-treated mice indicates that a fundamental mechanism of amyloid plaque formation has been disrupted. Subsequent studies indicate that Aβ production itself was unaffected (data not shown). $A\beta_{42}$ immunization therefore either prevents deposition and/or enhances the clearance of Aβ from the brain. The absence of neuritic and gliotic changes suggests that the $A\beta_{42}$-immunized mice never developed the neurodegenerative lesions that typify the progression of AD-like pathology in this model. The absence of enhanced astrocytosis, in particular, suggests that the processes preventing β-amyloidosis do not in themselves cause appreciable damage to the neuropil.

The above results clearly indicate that $A\beta_{42}$ immunization essentially prevents the development of AD-like neuropathology in the PDAPP mouse. It was unclear whether $A\beta_{42}$ immunization would improve the pathological outcome if treatment were initiated when a substantial Aβ plaque burden already existed. We therefore undertook further experiments in which immunizations with $A\beta_{42}$ began at an age when many β-amyloid plaques are already present in the brains of the PDAPP mice. Immunizations were continued during a period when the extent of Aβ deposition reaches levels comparable to those of established AD[11,12]. For this study, approximately 11-month-old, heterozygotic female PDAPP mice ($n = 24$) were immunized repeatedly with $A\beta_{42}$ plus adjuvant, with an injection protocol and schedule equivalent to those used in the young PDAPP mouse study (see Methods). Similar titre responses against $A\beta_{42}$ to those seen in younger animals were generated in the older animals. As a negative control, a parallel group of 24 transgenic littermates was immunized with PBS plus adjuvant. One-half of each group was killed at 15 months of age after 4 months' treatment, and the remaining half was killed at 18 months

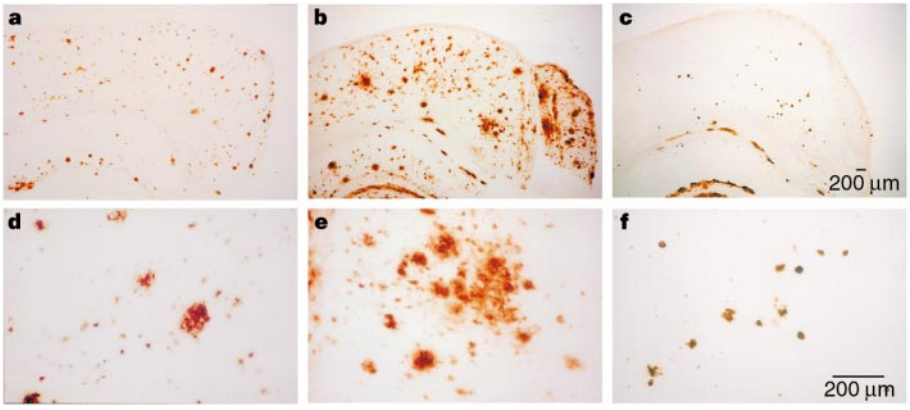

Figure 4 Reduction of cortical Aβ deposition in older PDAPP mice immunized with $A\beta_{42}$. Aβ deposits in the brains of 12-month-old untreated PDAPP mice and 18-month-old PBS- and $A\beta_{42}$-injected mice with median Aβ burdens representative of their respective treatment groups (see Fig. 3). **a**, Distribution of amyloid plaques in the frontal and retrosplenial cortices of a 12-month-old untreated PDAPP mouse, typifying the plaque burden of both PBS- and $A\beta_{42}$-injected groups at the start of the study. The plaques are shown at a high magnification in **d**. Compared with the 18-month PBS controls (**b**, **e**), Aβ deposits were significantly decreased in the 18-month $A\beta_{42}$-immunized group (**c**, **f**). Most of the cortical Aβ in brains of $A\beta_{42}$-injected mice was detected in small extracellular or cell-associated deposits (**f**) compared with the large and numerous extracellular deposits in the PBS group (**e**). Scale bar in **c** corresponds to **a**–**c**. Scale bar in **f** corresponds to **d**–**f**.

of age after 7 months' treatment. Groups of untreated PDAPP mice were also killed at ages 12, 15 and 18 months to serve as age-matched, non-immunized controls. At each time point, brains were examined by image analysis and enzyme-linked immunosorbent assay (ELISA) to determine the magnitude of the amyloid-β burden and the extent of neuritic dystrophy, astrocytosis and microgliosis.

Figure 3 shows the results of $A\beta_{42}$ treatment on cortical amyloid-β burden, determined by quantitative image analysis. The median value of cortical amyloid-β burden was 0.28% in untreated, 12-month-old PDAPP mice, a value representative of the plaque load in the experimental mice at the start of the study. At 18 months, the amyloid-β burden had increased by more than 17-fold to 4.87% in PBS-treated mice, while $A\beta_{42}$-treated mice had a greatly reduced amyloid burden of only 0.01%. The amyloid-β burden was significantly reduced in the $A\beta_{42}$ recipients at both 15 months (96% reduction; $P = 0.003$) and 18 months (>99% reduction; $P = 0.0002$). Figure 4 depicts the burden of amyloid-β in the 12-month-old PDAPP brain at the start of the experiment (Fig. 4a, d). At 18 months of age, the progression of Aβ-plaque pathology was obvious in the PBS group (Fig. 4b, e), but greatly diminished in the $A\beta_{42}$-injected mice (Fig. 4c, f). Compared with the 12-month-old untreated mice, several brains from the $A\beta_{42}$ group had fewer diffuse and mature amyloid-β deposits at 15 and 18 months, suggesting that the treatment had resulted in the clearance of pre-existing amyloid-β deposits (Fig. 4: compare a and d with c and f). Immunohistochemistry with anti-mouse immunoglobulin antibodies showed that the remaining plaques were often decorated with IgG in $A\beta_{42}$-treated but not in PBS-treated mice at both 15 and 18 months of age (data not shown).

Cortical amyloid-β deposition in PDAPP brains begins in the cingulate, frontal and retrosplenial cortices and progresses in a lateral–ventral fashion to sequentially involve the temporal and entorhinal cortices. After 3 months of treatment, amyloid-plaque pathology was diminished in the retrosplenial cortex (Fig. 5a, c) and completely absent in the entorhinal cortex (Fig. 5b, d) of the $A\beta_{42}$-injected mice. The progressive β-amyloidosis that would normally pervade the entorhinal cortex was thus halted by $A\beta_{42}$ immunization.

PDAPP mice also invariably develop heavy amyloid-β deposition in the outer molecular layer of the hippocampal dentate gyrus[11]. In a number of brains from $A\beta_{42}$-immunized mice, this pattern was considerably altered; the hippocampal deposition no longer contained diffuse amyloid-β deposits, and the banded pattern was completely disrupted (Fig. 6). Instead, unusual punctate structures were present that were reactive with anti-Aβ antibodies, and several appeared to be Aβ-containing cells (Fig. 6b). The pattern of apparent cellular labelling produced by the amyloid-β antibodies was replicated in adjacent sections by immunolabelling with antibodies directed at major histocompatibility complex (MHC) class II molecules (Fig. 6c). Phenotypically, these cells resembled activated microglia and monocytes and were occasionally found associated with the wall or lumen of blood vessels. They were not immunoreactive with antibodies that recognize T-cell (CD43, CD3e) or B-cell (CD45RA, CD45RB) surface markers (data not shown). No such cells were found in any of the PBS-treated mice.

Amyloid-β ELISA analysis of the older PDAPP mice was consistent with the immunohistochemical observations. In untreated PDAPP mice, the median level of total Aβ in the cortex at 12 months was 1,600 ng per g (wet weight); this had increased to 8,700 ng per g by 15 months[12]. At 18 months the value was 22,000 ng per g, an increase of more than 10-fold during the course of the experiment[12]. PBS-treated animals had comparable levels of total amyloid-β at 15 months (8,600 ng per g), and 19,000 ng per g at 18 months. In contrast, $A\beta_{42}$-treated animals had 81% less total amyloid-β at 15 months (1,600 ng per g) than the PBS-immunized group. Significantly less total amyloid-β (5,200 ng per g) was found at 18 months when the $A\beta_{42}$ and PBS groups were compared, representing a 72% reduction ($P = 0.0001$) in the amyloid-β that would have otherwise been present. Similar results were obtained when cortical levels of $A\beta_{42}$ were compared, namely that the $A\beta_{42}$-treated group contained much less $A\beta_{42}$, and the differences between the $A\beta_{42}$ and PBS groups were significant at 15 months ($P = 0.04$) and 18 months ($P = 0.0001$). In contrast, cortical levels of APP decreased by less than 10% of those in 12-month-old untreated animals (data not shown)[12]. These findings argue against the possibility that the reduction in amyloid-β deposition seen in the treated mice is due to an alteration in APP metabolism.

The progression of neuritic pathology was significantly reduced in the frontal cortex of $A\beta_{42}$-treated compared with PBS-treated mice (Table 1). At 15 months of age, the neuritic plaque burden in

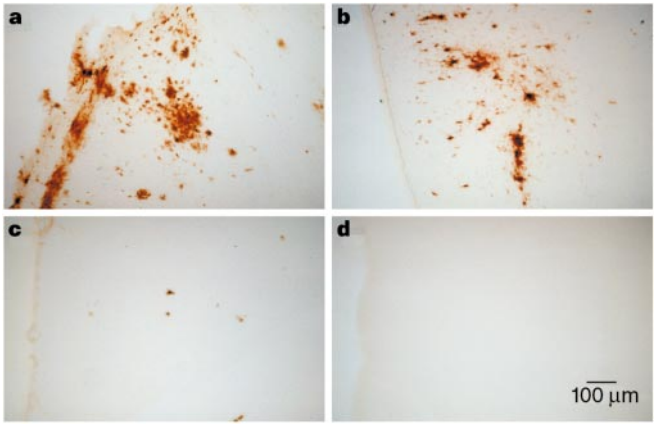

Figure 5 Reduction of Aβ burden in the entorhinal and retrosplenial cortex of older PDAPP mice following Aβ injection. Aβ deposition in the retrosplenial (RSC) and entorhinal (EC) cortices of 15-month-old PBS- (**a**, **b**) and $A\beta_{42}$- (**c**, **d**) injected mice with Aβ burdens representative of the median values of their respective groups. Aβ deposition was greatly reduced in the RSC of $A\beta_{42}$-injected mice compared with the PBS group (compare **a** and **c**). No Aβ was detected in the EC of $A\beta_{42}$-injected mice (**d**), in contrast to the PBS group (**b**). Scale bar in **d** corresponds to all panels.

Figure 6 Altered Aβ burden in the hippocampus of older $A\beta_{42}$-treated mice. Distribution of hippocampal Aβ in $A\beta_{42}$-injected brains (**b**), compared with the PBS group (**a**) at 18 months of age. In the PBS group, the characteristic appearance of diffuse (asterisk) and compacted (arrow) Aβ deposits was evident (**a**). This pattern was markedly altered in a number of $A\beta_{42}$-immunized mice (**b**), with the absence of diffuse deposits and an unusual punctate pattern of Aβ immunoreactivity associated with cells (**b**, arrow). The distribution of MHC II-labelled (Pharmigen) cells in a near-adjacent section (**c**) corresponded to the pattern of Aβ-positive cellular labelling shown in **b**. No such obvious cell Aβ staining was found in the PBS group (compare **a** and **b**). Scale bar in **c** corresponds to all panels.

Table 1 Image analysis of neuritic plaque and astrocytic burden in $A\beta_{42}$-treated PDAPP mice

	15 months		18 months	
	PBS	$A\beta_{42}$-treated	PBS	$A\beta_{42}$-treated
Neuritic plaque (%)	0.32	0.02	0.49	0.22
Astrocytosis (%)	4.26	1.89	5.21	3.20

Quantitative image analysis of neuritic plaques and astrocytosis was performed using antibody 8E5 to human APP and anti-GFAP, respectively. Methods are described in Fig. 1 legend. Reduction of neuritic plaque burden at ages 15 and 18 months by $A\beta_{42}$ treatment was statistically significant ($P = 0.03$ and 0.01, respectively), as was reduction of astrocytosis at the same time points ($P = 0.01$ and 0.03, respectively).

the $A\beta_{42}$-treated mice was reduced by 84% compared with the PBS group (0.05% and 0.32%; $P = 0.03$). Reduction in the neuritic-plaque pathology was similarly maintained between the two groups at 18 months of age, where the degree of neuritic dystrophy was reduced by 55% in the $A\beta_{42}$-treated mice (0.22% and 0.49%; $P = 0.01$).

Reactive astrocytosis was also significantly reduced in the retrosplenial cortex of $A\beta_{42}$-treated mice compared with PBS-treated mice at both 15 and 18 months of age. The per cent of astrocytosis in the PBS group increased between 15 and 18 months from 4.29% to 5.21%. $A\beta_{42}$ treatment suppressed the development of astrocytosis at both time points to 1.89% and 3.2%, respectively. These differences represent a 56% reduction ($P = 0.01$) at 15 months of age and a 34% decrease ($P = 0.03$) at 18 months of age in the $A\beta_{42}$-treated group.

In summary, immunization with $A\beta_{42}$ greatly reduced the development of the AD-like pathology that otherwise occurs in the PDAPP mouse. Immunization preceding plaque development profoundly affected the occurrence of new lesions, as the progression of β-amyloidosis and associated neuropathology was essentially wholly blocked, as seen both in the entire brain of the young animals and in at-risk brain regions of the older animals. Amyloid-β immunization also significantly retarded the progression of existing pathology in affected regions of the older animals. Outcomes of Aβ-plaque burden, neuritic dystrophy and gliosis were all significantly improved by $A\beta_{42}$ treatment in both young and old animals. In addition, the mechanism resulting in plaque reduction did not seem to produce any obvious signs of damage to the neuropil of $A\beta_{42}$-immunized animals. Histological examination of several organs, including brain and kidney, revealed no signs of immune-mediated complications, despite the high levels of human APP expressed in these tissues and the significant antibody titre to endogenous mouse Aβ peptide (data not shown).

To our knowledge, this is the first report of a clinically relevant treatment that reduces the progression of AD-like neuropathology in a transgenic animal model of the disease. Although it remains unproven, it is not unreasonable to expect that a similar reduction of neuropathology in AD patients would be of clinical benefit. Although our understanding of the precise aspects of the immune response that result in reduced pathology is incomplete, we have shown that $A\beta_{42}$ immunization results in the generation of anti-Aβ antibodies and that Aβ-immunoreactive monocytic/microglial cells appear in the regions of remaining plaques. Thus, one possible mechanism of action is that anti-Aβ antibodies facilitate clearance of amyloid-β either before deposition, or after plaque formation, by triggering monocytic/microglial cells to clear amyloid-β using signals mediated by F_c receptors.

It has been suggested that a chronic inflammatory state exists in the brain of patients with Alzheimer's disease: specifically the levels of complement, cytokines and acute-phase proteins are raised[14]. These observations have led to the hypothesis that anti-inflammatory regimens might be of therapeutic value. The findings presented here argue that an alternative approach, one that augments a highly specific immune response, can markedly reduce pathology in an animal model of the disease. Collectively, the results suggest that amyloid-β immunization may prove beneficial for both the treatment and prevention of Alzheimer's disease. □

Methods

Immunization procedures. Aβ peptide was freshly prepared from lyophilized powder for each set of injections. For immunizations, 2 mg $A\beta_{42}$ (human $A\beta_{1-42}$; US Peptides) was added to 0.9 ml deionized water and the mixture was vortexed to generate a relatively uniform suspension. A 100-μl aliquot of 10 × PBS (where 1 × PBS is 0.15 M NaCl, 0.01 M sodium phosphate, pH 7.5) was added. The suspension was vortexed again and incubated overnight at 37 °C for use the next day. Serum amyloid-P component immunogens were prepared using mouse SAP amino acids 77–85 and 164–173, each conjugated to sheep anti-mouse IgG (Jackson Immunochemicals) as described[15]. $A\beta_{42}$ or SAP peptides (100 μg antigen per injection) were emulsified 1:1 (v/v) with complete Freund's adjuvant for the first immunization, followed by a boost in incomplete Freund's adjuvant at 2 weeks, and monthly thereafter. $A\beta_{42}$ or SAP in PBS alone was injected from the fifth immunization onward. Titres were determined by serial dilutions of sera against either aggregated $A\beta_{42}$ or SAP protein which had been coated onto microtitre wells. Detection used goat anti-mouse immunoglobulin conjugated to horseradish peroxidase and slow-TMB (3,3″,5,5′-tetramethyl benzidine; Pierce) substrate. Titres were defined as the dilution yielding 50% of the maximal signal.

Neuropathology quantification. To quantify amyloid burden, PDAPP mouse brain tissue was fixed in 4% paraformaldehyde, cut to 40-μm coronal sections and reacted with an anti-Aβ biotinylated antibody, 3D6, as described previously[11]. Quantitative image analysis was performed using a Videometric 150 Image Analysis System (Oncor) linked to a Nikon Microphot-FX microscope through a CCD video camera. The image of the immunoreacted section was stored in a video buffer and a specific brain region (hippocampus or cortex) was manually outlined and the total pixel area occupied by the structure determined. A monochromatic-based threshold was set to select pixels corresponding to immunolabelled structures. The per cent of the brain region occupied by the labelled pixels was then calculated. For all image analyses, six sections at the level of the dorsal hippocampus, each separated by consecutive 240-μm intervals, were evaluated for each animal. In all cases, the treatment status of the animals was unknown to the observer. Mann–Whitney nonparametric analysis was performed using Statview software (SAS Institute, Cary, NC). Similar methodologies were used to quantify neuritic dystrophy and gliosis. Specific reagents are indicated in the appropriate figures.

Received 6 April; accepted 5 May 1999.

1. Hyman, B. T. New neuropathological criteria for Alzheimer disease. *Arch. Neurol.* **55,** 1174–1176 (1998).
2. Tanzi, R. E. *et al.* The gene defects responsible for familial Alzheimer's disease. *Neurobiol. Dis.* **3,** 159–168 (1996).
3. Hardy, J. New insights into the genetics of Alzheimer's disease. *Ann. Med.* **28,** 255–258 (1996).
4. Citron, M. *et al.* Mutation of the β-amyloid precursor protein in familial Alzheimer's disease increases β-protein production. *Nature* **360,** 672–674 (1992).
5. Scheuner, D. *et al.* Secreted amyloid β-protein similar to that in the senile plaques of Alzheimer's disease is increased *in vivo* by the presenilin 1 and 2 and APP mutations linked to familial Alzheimer's disease. *Nature Med.* **2,** 864–870 (1996).
6. Suzuki, N. *et al.* An increased percentage of long amyloid β protein secreted by familial amyloid β protein precursor (β APP717) mutants. *Science* **264,** 1336–1340 (1994).
7. Citron, M. *et al.* Mutant presenilins of Alzheimer's disease increase production of 42-residue amyloid β-protein in both transfected cells and transgenic mice. *Nature Med.* **3,** 67–72 (1997).
8. Borchelt, D. R. *et al.* Familial Alzheimer's disease-linked presenilin 1 variants elevate Aβ1-42/1-40 ratio *in vitro* and *in vivo*. *Neuron* **17,** 1005–1013 (1996).
9. Iwatsubo, T. *et al.* Visualization of Aβ42(43) and Aβ40 in senile plaques with end-specific Aβ monoclonals: evidence that an initially deposited species is Aβ42(43). *Neuron* **13,** 45–53 (1994).
10. Lippa, C. F., Nee, L. E., Mori, H. & St George-Hyslop, P. Aβ-42 deposition precedes other changes in PS-1 Alzheimer's disease. *Lancet* **352,** 1117–1118 (1998).
11. Games, D. *et al.* Alzheimer-type neuropathology in transgenic mice overexpressing V717F β-amyloid precursor protein. *Nature* **373,** 523–527 (1995).
12. Johnson-Wood, K. *et al.* Amyloid precursor protein processing and Aβ42 deposition in a transgenic mouse model of Alzheimer disease. *Proc. Natl Acad. Sci. USA* **94,** 1550–1555 (1997).
13. Liang, J. S. *et al.* Evidence for local production of acute phase response apolipoprotein serum amyloid A in Alzheimer's disease brain. *Neurosci. Lett.* **225,** 73–76 (1997).
14. McGeer, E. G. & McGeer, P. L. The role of the immune system in neurodegenerative disorders. *Mov. Disorders* **12,** 855–858 (1997).
15. Seubert, P. *et al.* Isolation and quantification of soluble Alzheimer's β-peptide from biological fluids. *Nature* **359,** 325–327 (1992).
16. Seubert, P. *et al.* Secretion of β-amyloid precursor protein cleaved at the amino terminus of the β-amyloid peptide. *Nature* **361,** 260–263 (1993).

Acknowledgements. We thank Rae Lyn Burke for helpful comments.

Correspondence and requests for materials should be addressed to D.S. (e-mail: dschenk@elanpharma.com).